CHAPTER 5

DISCUSSION

5. 1 S-Type and I-Type Granites

Chappell and White (1974) suggested, on the basis of field evidences, petrological and geochemical data, that various granitic rocks in the southeastern Australia might have been derived from either sedimentary source rocks (S-type granites) or from igneous source rocks (I-type granites). The principal characteristics of the two contrasting granite types are summarized in Table 5.1.

Ishihara (1977) classified the granitoids into 2 series; the magnetite-series granitoids contain an easily recognizable amount of magnetite under the microscope, whereas the ilmenite-series rocks are practically free of opaque oxide minerals (less than 0.1 vol %), in which ilmenite is consistently seen. They can be distinguished by means of their different magnetic susceptibilities, the magnetite-series rocks showing high values (more than 100×10^{-6} emu/g) and the ilmenite-series ones showing low values (less than the above figure) (Takahashi et al., 1980). Ishihara (1980) also poined out that tin deposits are associated almost exclusively with ilmenite-series whereas tungsten deposits can be associated with both ilmenite and magnetite-series.

It should be noted that the S - and I-type classification has the genetic implication, but the classified rocks are mineralogically somewhat similar to the descriptive classification of the ilmenite-and magnetite-series, respectively. However, Ishihara et

Table 5.1 Principal characteristics of S - and I - type granites (modified after Chappell and White, 1974; Hine et al., 1978)

S - types	I - types
(1) Relatively low sodium, Na_2O normally $< 3.2\%$ in rocks with approx. 5% K_2O, decressing to $< 2.2\%$ in rocks with approx. 2% K_2O	(1) Relatively high sodium, Na_2O normally $> 3.2\%$ in felsic varieties decreasing to $> 2.2\%$ in more mafic types
(2) Mol. $Al_2O_3/ (Na_2O + K_2O + CaO) > 1.1$	(2) Mol. $Al_2O_3/(Na_2O + K_2O + CaO) < 1.1$
(3) $>$ 1% CIPW normative corundum	(3) CIPW normative diopside or $<$ 1% CIPW normative corundum
(4) Relatively restricted in composition to high SiO_2 types	(4) Broad spectrum of compositions from felsic to mafic
(5) Variation diagrams irregular	(5) Regular inter-element variations within plutons; linear or near linear variation diagrams
(6) High initial $^{87}Sr/^{86}Sr$ ratios (> 0.708)	(6) Low initial $^{87}Sr/^{86}Sr$ ratios (< 0.708)
(7) Biotite abundant in more mafic types, up to 35%, and muscovite is common in more felsic types	(7) Hornblende is common in more mafic types and generally present in felsic types.
(8) Common accessory minerals include monazite, ilmenite and alumino-silicates such as garnet and cordierite, etc.	(8) Usually contain primary sphene, allanite and magnetite
(9) Hornblend-bearing xenoliths are rare but metasedimentary xenoliths are not uncommon	(9) Mafic hornblende bearing xenoliths of igneous appearance are common

al. (1980) subsequently pointed out that the ilmenite-series consist of both the S-type and the I-type.

The initial $^{87}Sr/^{86}Sr$ ratio data of the porphyritic biotite granites of the Khuntan Mountain Range (see Figure 1.2) reported by Teggin (1975), Braun et al. (1976), Beckinsale (1979), and Nakapadungrat (1982) (see also Geochronology of granitic rocks in Chapter 2) reveal that all Triassic granites are the S-type with a very high initial $^{87}Sr/^{86}Sr$ ratio ranging from 0.7244 ± 0.0020 to 0.7295 ± 0.0007. Thus, it is reasonable to believe that the porphyritic biotite granites of the Mae Chedi (GR-1), which is a part of the Khuntan Mountain Range, is the S-type and possesses the same range of $^{87}Sr/^{86}Sr$ initial ratio.

The chemical data of the Mae Chedi granites are summarized in accordance with the chemical criteria proposed by Chappell and White (1974) and shown in Table 5.2. Although there is the absence of actual initial $^{87}Sr/^{86}Sr$ value, the data in Table 5.2 strongly suggest that all of the analyzed granites are peraluminous and can be classified as the S-type granites (only the GR-3 have an average Na_2O contents higher than 3.2 % (3.36 %). It can, therefore, be concluded that tin and tungsten deposits of the Mae Chedi Mine are possibly associated with the S-type granites. A similar suggestion of Plimer (1980) that the tin and tungsten deposits in many places, e.g. Cornwall, U.K.; Erzgebirge district, East Germany and Czechsolvakia; and the Wolfram Camp, Herberton and New England districts of Australia, are associated with the S-type granites though Chappell and White (1974) suggested that tin is associated

with the S-type granites whereas tungsten and porphyry-type copper and molybdenum deposits are associated with the I-types. In their previous study in the Mae Chedi Mine (Khun Plin Mine), Suensilpong and Jungyusuk (1981) have also come to the same conclusion that tin and tungsten are associated with the S- and the I-type granites, respectively. However, the result of the present study indicates that tin as well as tungsten are conclusively associated with the S-type granites.

Table 5.2 Geochemical criteria of Chappell and White (1974) applied to the Mae Chedi granites.

Rock Types	No.of Samples	Na_2O %	K_2O %	Mol.Al_2O_3/ (Na_2O + K_2O + CaO)	Norm C (%)
GM-1	6	2.87	4.51	1.24	3.29
GM-2	6	3.12	5.07	1.22	2.81
GM-3	3	2.68	5.63	1.28	3.41
GR-1	4	2.84	4.81	1.15	2.02
GR-2	2	2.97	4.87	1.20	2.34
GR-3	4	3.36	4.83	1.15	1.81

5. 2 CIPW Norms and Their Plots in the System Quartz-Albite-Orthoclase-H_2O

CIPW norms of the Mae Chedi granites are calculated and shown in Table 4.1. Normative quartz, albite, and orthoclase are

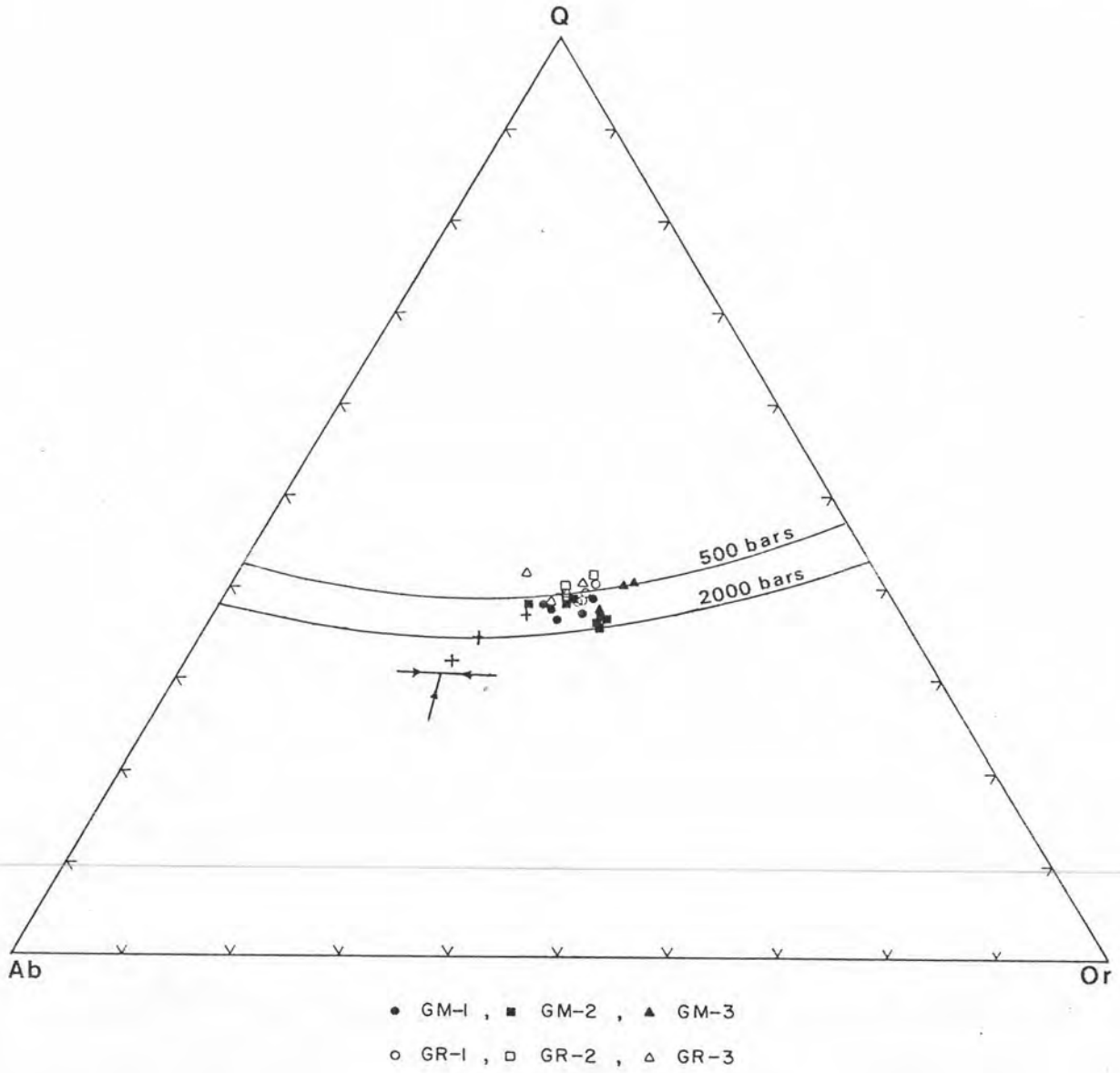

Figure 5.1 Normative Q-Ab-Or diagram for the Mae Chedi granites. The quartz - feldspar field boundaries at 500 and 2000 bars P_{H_2O}, and positions of quaternary isobaric minima are from Tuttle and Bowen (1958).

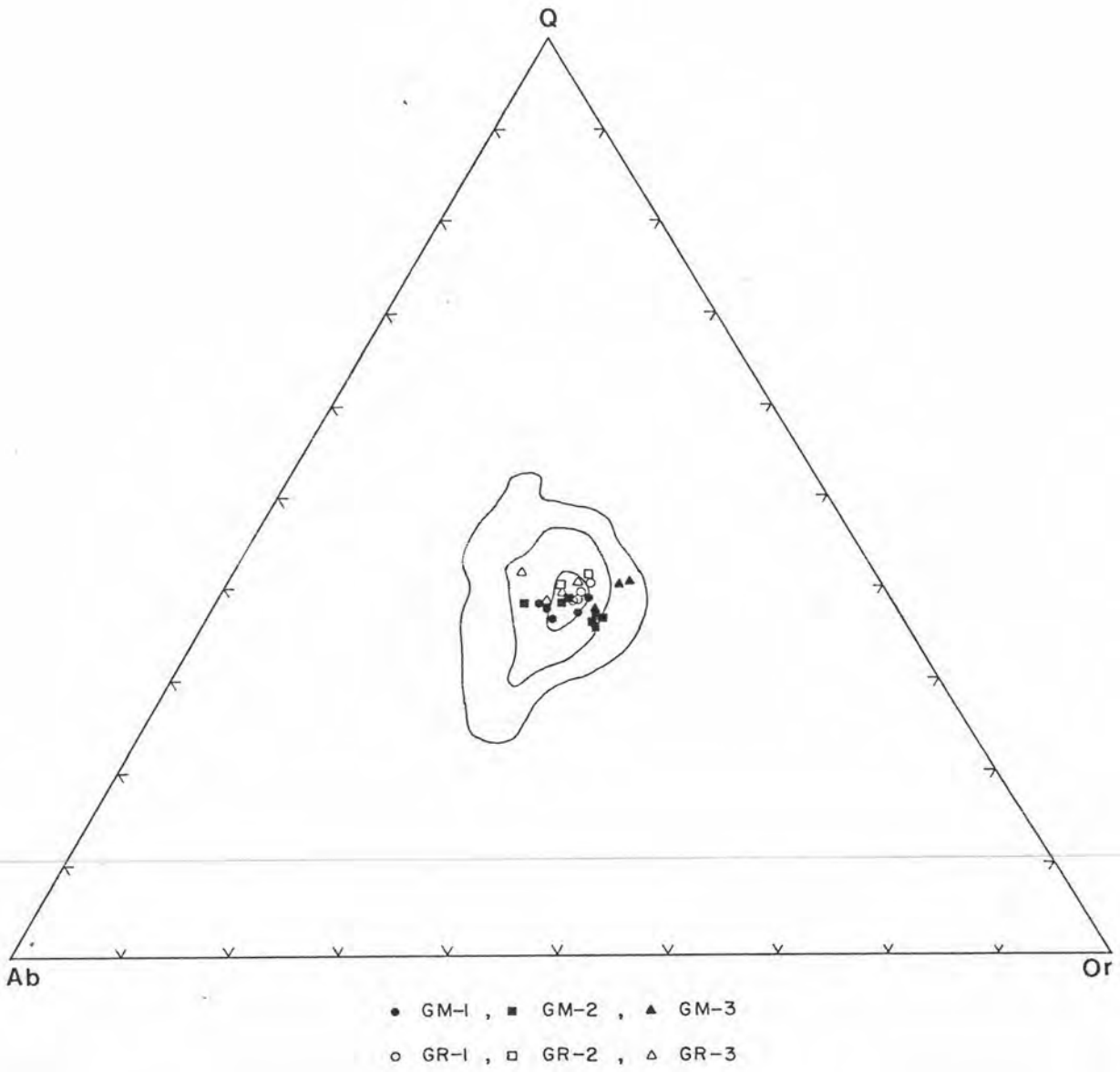

Figure 5.2 Contour diagram showing the frequency distribution of normative quartz, albite, and orthoclase in Washington's (1917) plutonic rock tables to compare with the Mae Chedi granites. Contours more than 5, 10, and 15 percent in a 1 percent area (after Luth et al., 1964).

recalculated at 100 percent and plotted on the experimentally derived phase diagrams in the systems Q-Ab-Or-H_2O (after Tuttle and Bowen, 1958) as shown in Figure 5.1

From Figure 5.1, it is obvious that the sample plots of the GR-series tend to cluster on the quartz-feldspar field boundary which are close to the ternary mininum at low water pressure (about 500 bars) whereas alomost all the sample plots of the GM-series concentrate between the quartz-feldspar field boundaries at 500 and 2000 bars (about 1000 bars) which is the indicative of higher water pressure. Both of them seem to be a relatively restricted composition field in the system. However the fine- to medium-grained leucocratic granite GM-3 generally contains higher normative orthoclase, instead of albite, than the fine-grained biotite granite (GM-1) which indicates that the process of K-feldspathization might have taken place during the late magmatic crystallization.

A contour diagram in Figure 5.2 displays the frequency distributions of the normative quartz, albite, and orthoclase in 281 plutonic rocks, which contain normative corundum (alumina oversaturated), from Washington's (1917) table in comparison with the normative quartz, albite, and orthoclase of the Mae Chedi granites. The present data show that most of the Mae Chedi granites are coincident with those of the highest frequency distribution of plutonic rocks with having normative corundum (Luth et al., 1964).

5. 3 Model of Granitic Systems

The K/Rb ratios have long been suggested as a useful guide for the understanding of a magmatic differentiation. Since the

variation in the K/Rb ratio can be used to distinguish different types of granites which have similar mineralogy and major element contents, and can also be used to delineate the sequence of igneous intrusion (Taylor, 1965). Taylor (op. cit.) also, mentioned that, for a single fractionation sequence, the K/Rb ratio is likely to decrease toward the acid end of the sequence. Based on the consideration of the K/Rb as well as the Ba/Rb ratios and SiO_2 content of the GM- and the GR-series (Figure 4.6), it is suggested that the parent magma of the GR-series has fractionated from the GR-1 to the GR-2 and finally to the GR-3 in accordance with the decreasing of both the K/Rb and the Ba/Rb ratios. These patterns are in general aggreement with those studied by Taylor (op. cit.), Tauson and Kozlov (1973), Charusiri (1980), Charusiri and Pongsapich (1982), and Nakapadungrat (1982). In addition,the Li/Mg ratios are also useful, from the differentiation point of view, for the GR-granitic series. Despite of the decrease in lithium content from the GR-1 to the GR-3, magnesium content also decreases at a higher order of magnitude (Figures 4.1, 4.5). As a consequence, the Li/Mg ratio still increases as the differentiation progresses. This is also similar to the differentiation of the Samoeng granites (Punyaprasiddhi, 1980). In contrast to the GR-series, the GM-series do not follow the differentiation trends as those observed to the GR-series. The GM-series have higher K/Rb, Ba/Rb, and F/Li and lower K/Ba, Ca/Sr, Rb/Sr, and Li/Mg ratios than those of the GR-series (as shown in Figures 4.6, 4.7) suggesting that the variations of these elemental ratios of the GM-series may be resulted from the hydrothermal alteration process instead of the differentiation process.

Table 5.3 Partition coefficients (crystal/liquid) used in this study.

Element	Alkali feldspar	Plagioclase	Biotite
Rb	0.659[a]	0.048[a,b]	3.26[a,b]
Sr	3.870[a]	2.804[a,b]	0.12[a,b]
Ba	6.120[a]	0.360[a,b]	6.36[a,b]

Source : a. Schnetzler and Philpotts (1970), b. Philpotts and Schnetzler (1970).

The trace contents of Rb, Sr, and Ba are particularly useful for modelling the granitic systems since they occur only in the major silicate minerals but not in the accessory components (McCarthy and Hasty, 1976). The change in composition of liquid phase resulting from fractional crystallization of the solid phases may be calculated by the Rayleigh fractionation law, applied by Neuman et al. (1954) and Greenland (1970), as the following equations:

$$\frac{C_L}{C_0} = F^{(D_1 - 1)}$$

$$F = \frac{100 - \text{percentage of crystallization}}{100}$$

where C_L is the concentration of a trace element in the liquid after removal of the crystal, C_0 the original concentration of that element in the liquid, D_1 the partition or distribution coefficient (crystal/

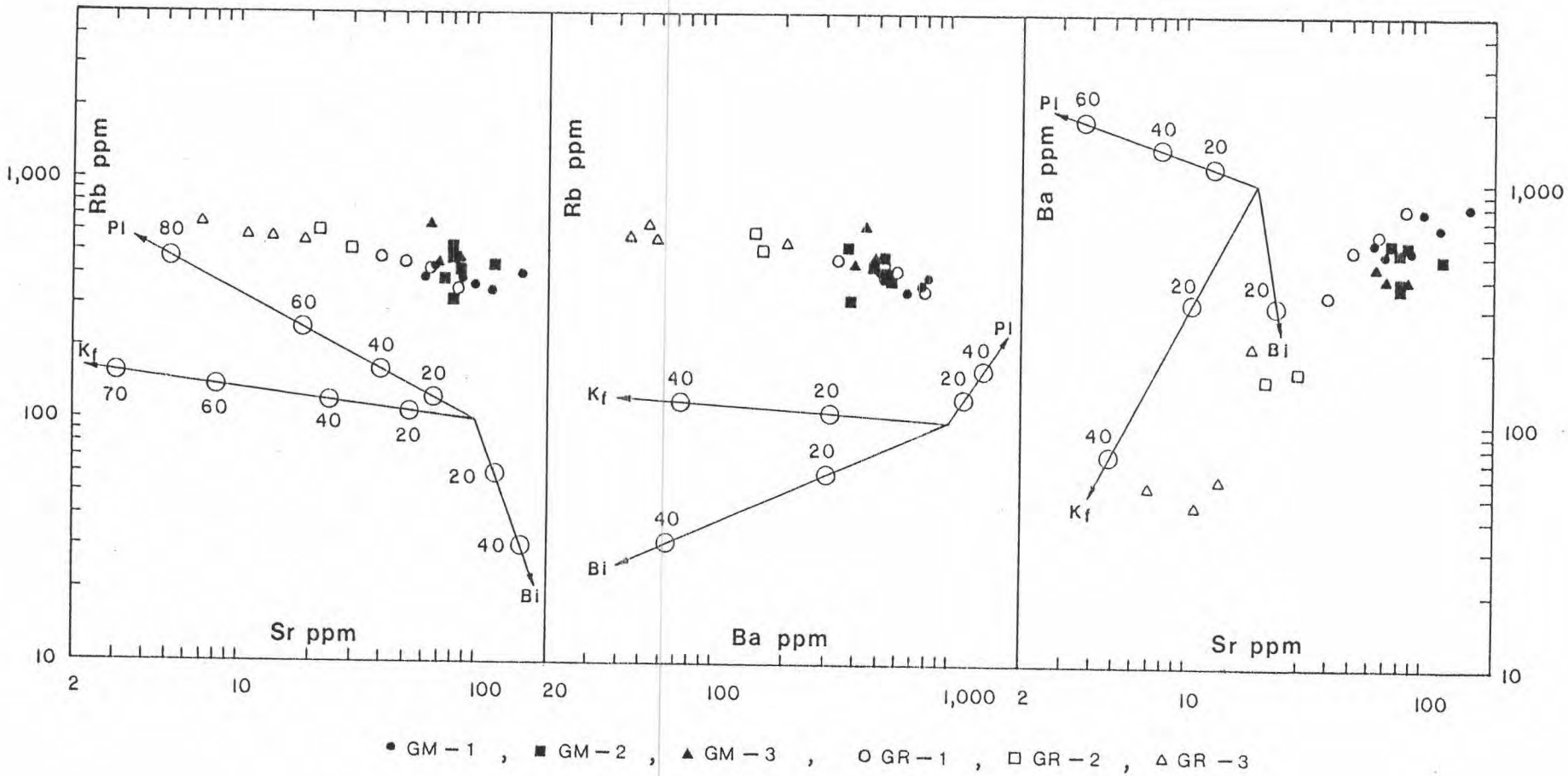

Figure 5.3 Interelement correlations of Rb, Sr, and Ba for the Mae Chedi granites. The mineral vectors indicate the change in composition of liquid phases as a result of fractional crystallization of the solid phases plagioclase (Pl), alkali feldspar (K_f), and biotite (Bi), calculated by the Rayleigh fractionation law, applied by Neuman et al. (1954) and Greenland (1970), using the distribution coefficients from Table 5.3. Numbers marked on the mineral vectors show the percentages of crystallization.

liquid), and F the fraction of remaining liquid. Based on the above equations and partition coefficients tabulated in Table 5.3, the results obtained in model calculations of perfect fractional crystallization are illustrated in Figure 5.3.

The Rb - Sr, Rb - Ba, and Ba - Sr data plots of the Mae Chedi granites (Figure 5.3) clearly show that the GR-series have developed a well-defined differentiation trend starting from the GR-1 to the GR-2, and finally to the GR-3, parallel to the vector of alkali feldspar. It is indicated the Rb, Sr, and Ba contents may have been influenced by crystal fractionation of alkali feldspar rather than plagioclase and biotite. On the contrary, these plots of the GM-series exhibit a cluster appearance. In terms of these distribution patterns, it is suggested that the variations of the GR-granitic series could be the result of fractional crystallization and the GR-3 type represents the crystallization of the ultimate granitic residual liquid of the series. In contrast, those of the variations of the GM-granitic series could be the result of metasomatic alteration and the GM-3 represents the ultimate metasomatic alteration product of the series.

Judging from the petrochemistry of the granitic rocks, it has clearly seen that the GM-series are unlikely related to the GR-series. Owing to the lack of the field relationship and the radiometric dating of both granitic series, the age relationship of these two granitic suites is still uncertain. However, Suensilpong and Jungyusuk (1981) suggested that fine-grained biotite granites of the Mae Chedi Mine (including Samoeng and Doi Mok Mines) are younger than porphyritic biotite granite of Upper Triassic age.

5. 4 Genetic Model of Tin-Tungsten Mineralizations

Although the primary tin-tungsten mineralizations occur in the Mae Chedi area where small granitic plutons of the GM-series intruded metabasites (Fingure 2.2), on the basis of the very low tin and tungsten contents of the metabasites (Table 4.5), it is reasonable to believe that the metabasites are not genetically associated with the tin-tungsten mineralizations, but they may act as a cap-rock. Furthermore, based on the field evidences and detailed petrochemical study of the granitic rocks, it may be that tin and tungsten mineralizations were introduced by hydrothermal fluids that moving upward through the N - S fracture systems developed in the GM-granitic series and were trapped under the metabasites. Contemporanously, reactions between the mineralized fluids and the wall rocks took place resulting in various kinds of wall-rock alterations such as K-feldspathization, tourmalinization, chloritization, sericitization, muscovitization, and albitization. The original source of tin and tungsten in the ore-forming fluids are still obscured. Based on the higher concentration of Sn and W in the GM-1 as compared with the GR-1 (see Tables 4.3, 4.4; Figure 4.5) or the world average for granites (2-3 ppm Sn, Hamaguchi and Kuroda, 1969, and probably 1-2 ppm W, Evans and Krauskopf, 1970, cited in Alderton and Moore, 1981), lead to suggest that the tin and tungsten may probably originate from the trace elements in the mineral constituents of the GM-1 granitic rocks such as biotites (Hesp, 1971; Groves 1972; Imeokparia, 1982). However, the rather high concentration of tin and tungsten in the GM-1 and the GM-2 may be

probably caused by the contamination of the ore forming fluids. By analogy with similar ore deposits elsewhere, the D/H analyses on muscovites from the Mae Lama hydrothermal vein system in northwestern Thailand have proved that meteoric water is involved in the formation of primary tungsten-tin deposit (Harmon and Beckinsale, unpublished, cited in Beckinsale, 1979). Nevertheless, the original source of tin and tungsten is also still uncertain. Beckinsale (1979) raised this point of view that whether the interaction with meteoric water is perhaps only an extra stage in concentrating ore metals derived from the granite, or the meteoric water that gained access to the cooling pluton contained dissolved ore components before interaction with a granite which acted only as a heat source to drive the hydrothermal circulation.

Of interesting field evidences are that cassiterite is chiefly confined to the uppermost part of the granitic pluton, while scheelite is commonly abundant towards the lower level, and, that scheelite in the ore veins occurs at the central zone and is symmetrically selvaged by cassiterite (Figure 5.4). Furthermore, some of cassiterite and tungsten minerals may tend to occur separately in veins. These lines of evidence lead to suggest that tin mineralization at the Mae Chedi Mine is not contemporaneous with tungsten. It is, therefore, envisaged that tin mineralization is more intensive in the first episode of hydrothermal activity and tungsten mineralization presents a later phase. A similar finding was also obtained from the studies of tin and tungsten mineralizations at the Samoeng Mine (Punyaprasiddhi, 1980; Suensilpong and Jungyusuk, 1981). In addition, Punyaprasiddhi (1980) proposed the tin

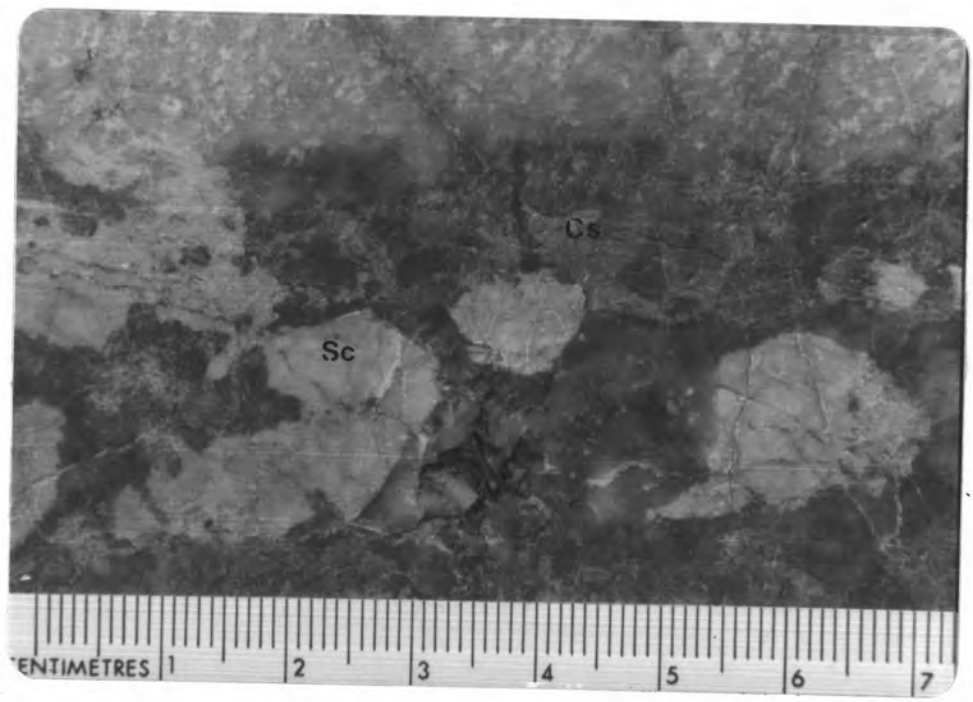

Figure 5.4 Photographs showing scheelite (Sc) occurring at the central zone of an ore vein which symmetrically selvaged by cassiterite (Cs).

mineralization at the Samoeng Mine is more concerned with the Triassic granite (S-type) while tungsten mineralization represents a later mineralizing phase probably in the Cretaceous. Suensilpong and Jungyusuk (1981), again, pointed out that tin is in a closer association with the porphyritic biotite granite (S-type) of Upper Triassic age, and scheelite is related to fine-grained biotite granites (I-type) which are younger age and different phase of the former granitic rock.

Scheelite deposits of northern Thailand are found mainly in contact zones between granitic rocks and calcareous rocks, e.g. Doi Mok Mine (German Geological Mission, 1972; Jivathanond, 1981), Samoeng Mine (Punyaprasiddhi, 1980), Mae Lama Mine (Suensilpong, 1975; Panupaisal, 1977; Pitragool and Panupaisal, 1979). These field evidences lead to suggest that the Ca in the scheelite may have been originated from the calcareous country rocks. However, in the case of the Mae Chedi area, no outcrops of calcareous rocks were observed in the nearby area of the scheelite deposits. Because of remarkably decreasing in anorthite contents in plagioclases of the GM-2 and the GM-3 as compared with the GM-1 (Table 3.1) and some scheelite grains are spatially associated with albitic plagioclase (Figure 3.11), it would be reasonable to suspect that the major Ca which is used to form scheelite may have been drawn from the formerly more calcic plagioclase of the GM-1 during the albitization. This conclusion is also supported by chemical analyses of the rocks (Tables 4.1, 4.2; Figure 4.1), which reveal that the CaO contents of the GM-granitic series decrease distinctively from the GM-1 to the GM-2 or the GM-3.